光学学报

基于脉冲串飞秒激光的血凝块消蚀效果研究

刘骁征[1]，李有楠[2]，张海涛[3**]，顾瑛[1,4*]，吴巍巍[2]，张童[2]

[1]北京理工大学光电学院，北京 100081；

[2]清华大学附属北京清华长庚医院血管外科，清华大学临床医学院，北京 102218；

[3]清华大学精密仪器系激光与光子技术研究室，光子测控技术教育部重点实验室，北京 100084；

[4]中国人民解放军总医院第一医学中心激光医学科，北京 100853

摘要 脉冲串飞秒激光在工业精密加工中展现出低热高效的特性，有望为血栓清除技术提供新型解决方案。以动物血凝块为消蚀样本，将脉冲串飞秒激光与高速振镜相结合来搭建实验平台，对样本表面进行单层扫描消蚀，使用三维超景深显微镜对消蚀坑进行观察和记录，并与相同平均功率下的传统脉冲模式飞秒激光的消蚀结果进行比较。结果表明，相比于传统脉冲模式，脉冲串飞秒激光可以提升消蚀效率并降低消蚀阈值，具有良好的临床研发潜力。

关键词 医用光学；飞秒激光；组织消蚀；脉冲串模式；三维显微成像

中图分类号 R454.2；TN249 **文献标志码** A **DOI**：10.3788/AOS221371

1 引 言

血栓栓塞或血栓形成是动脉闭塞性疾病的重要成因[1]。快速清除血栓、恢复动脉血流是治疗动脉血栓性疾病的关键策略之一。目前，清除动脉血栓的手段主要包括药物治疗和手术治疗[2-4]。部分急性期血栓可采取全身药物溶栓的方式来清除，大部分血栓清除仍需借助手术。传统开放手术使用取栓导管移除血栓，但有一定手术创伤。微创手术通过溶栓导管或血栓清除装置清除血栓，手术创伤较小，但现有器械仍存在血栓清除率低、可能引起血管壁损伤破裂等不足[5]。因此，研发新型血栓清除装置具有重要的临床意义。

飞秒激光作用于物质上的时间尺度为飞秒至亚皮秒量级，小于脉冲激光发生热消蚀的临界时间尺度（1～10 ps）[6]，且极高的瞬时峰值功率会诱导物质表面形成等离子体[7]。表面等离子体可以对激光能量进行非线性强吸收，并通过电子-声子耦合作用对局部区域物质进行快速热化从而实现物质消蚀，可有效避免对周围物质造成热损伤[8]，故飞秒激光被广泛应用于金属[9-11]、半导体[12-13]和医用有机材料[14-16]等材料的精密加工中，且几乎均能实现边缘锐利、无明显裂纹碎片的高质量加工结果。飞秒激光优异的消蚀特性使其具备良好的医疗研发潜力，但是目前仍存在一定的局限性。为了提高飞秒激光的消蚀效率，提高脉冲能量密度是一种可行的方式。然而，该方式会导致消蚀结果的质量下降[17]，出现热熔烧蚀[18]、裂纹[19]和基底崩裂[20]等现象，说明此时会出现严重的热沉积，故在医疗应用中可能会产生热损伤等现象，而脉冲串飞秒激光有效解决了这一问题。

脉冲串模式与传统模式不同，传统模式每周期输出的是单脉冲，而脉冲串模式每周期输出的是脉冲序列，故在时域上脉冲串模式具有脉冲串内高重复频率提升消蚀效率和脉冲串间低占空比提供足够冷却时间的特性[21]。Butkus等[22]使用脉冲串飞秒激光器对因瓦合金箔进行消蚀钻孔，与相同平均功率密度下的传统脉冲模式相比，消蚀效率提高了一个数量级，且消蚀孔洞边缘光滑。在其他脉冲串飞秒激光参数下，硅[23]、不锈钢[24]和铜[25]等材料的消蚀实验中消蚀效率也得到了有效提升，并且有效抑制了热效应。Kerse等[26]使用脉冲串飞秒激光与传统脉冲模式飞秒激光进行了对比：在人牙本质消蚀实验中，相同平均功率密度下脉冲串模式的消蚀效率为传统脉冲模式的6倍，且平均功率密度较高时，传统脉冲模式结果中出现碳化现象而脉冲串模式仍保持光滑的消蚀边缘；在进一步实验中对小鼠脑组织进行消蚀，通过病理检测发现，脉冲串模式下小鼠脑组织的消蚀边缘清晰，无热损伤，而传统脉冲模式下小鼠脑组织消蚀边缘模糊，边缘细胞失去生物活性。因此，脉冲串飞秒激光具有低热高效的优良消蚀效果，有望成为新型血栓清除手段。

目前鲜有关于脉冲串飞秒激光消蚀血栓的研究报道，缺乏实验数据来验证脉冲串飞秒激光消蚀血栓的

收稿日期：2022-06-27；**修回日期**：2022-07-07；**录用日期**：2022-07-14；**网络首发日期**：2022-07-24

通信作者：*guyinglaser301@163.com；**zhanghaitao@mail.tsinghua.edu.cn

实际效果。因此，本文将高速扫描振镜和脉冲串飞秒激光器结合搭建了实验平台，激光器脉冲时序可调，可切换脉冲串模式与传统脉冲模式，以动物血凝块为消蚀样本进行体外消蚀实验，使用三维超景深显微镜对消蚀坑进行观察和记录，并与相同平均功率密度下的传统脉冲模式飞秒激光的消蚀结果进行比较，以评估各激光参数下脉冲串飞秒激光对血凝块的消蚀效果。

2 实验方法

整体实验装置组成示意图如图 1 所示，采用波长为 1030 nm、脉冲宽度为 250 fs 的飞秒激光器，具备传统模式和脉冲串模式，脉冲和脉冲串重复频率均可调，光路中光束直径由光阑 D1 和 D2 调整为 7 mm，利用全反射镜 M1 和 M2 进行光路折叠和准直，之后光束进入高速激光振镜输入窗口。高速激光振镜采用 RAYLASE 的 SS-III-15[Y] D2 AC 两轴激光扫描振镜，输入窗口直径为 14 mm，利用内部的一组高速反射镜使输出光束快速改变方向从而实现扫描。利用场镜聚焦振镜输出光束再进行输出，实验选用的场镜的焦距为 100 mm，焦平面扫描范围为 50 mm×50 mm，使用感光相纸实测得到的聚焦光斑的直径为 100 μm。

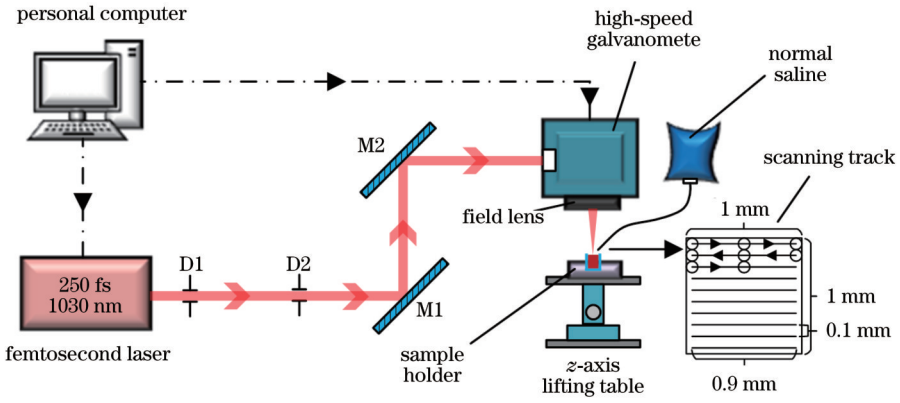

图 1 整体实验装置图

Fig. 1 Overall experimental device diagram

实验采用市场购买的新鲜可食用鸭血凝块作为消蚀样本，实验时将装有血凝块样本的玻璃管插入固定在 z 轴升降台上的样本支架中，通过调整 z 轴升降台的高度实现高速激光振镜输出的聚焦光束聚焦于体外血栓样本的表面上。在消蚀实验过程中滴加生理盐水以模拟体液环境。由于单照射点消蚀效果不明显，故为了便于检测和观察，采用单层大面积扫描的方式进行消蚀实验，扫描轨迹如图 1 所示，每次实验仅扫描一次形成单层消蚀坑，扫描轨迹全长 9 mm，扫描光场覆盖面积为 1 mm×1 mm。消蚀实验结果采用基恩士 VHX-6000 超景深三维显微镜观察并记录消蚀数据，选择放大倍数为 100，以获得消蚀坑显微图像和消蚀形貌数据。

实验分组如表 1 所示，共进行 12 组实验，每组进行 3 次。1～6 组为脉冲串模式实验组，一个脉冲串内含有 5 个子脉冲，相邻子脉冲的重复频率为 1 MHz，相邻脉冲串的重复频率为 1 kHz 或 2 kHz，如图 2(a)、(b)所示。7～12 组为传统模式实验组，脉冲重复频率为 5 kHz 或 10 kHz，如图 2(c)、(d)所示。

本文采用等效能量密度对实际照射的能量密度进行简化描述。在较小扫描面积下，圆形光斑面积和矩形扫描面积的差异不可忽略，但随着扫描面积的扩大，扫描光场边缘处的圆形光斑边界带来的照射面积差异几乎可忽略不计。以实验组 1 为例，由光斑圆形边缘引起的能量密度差异为 2.2%，故本文采用的等效能量密度可对照射情况进行简化描述。此外，在实验时，要求血凝块厚度均为 5 mm，并要求上表面与实验平台几乎平行，从而确保对焦位置基本相同，使得所有样品在相同参数的照射下所接收的能量密度一致。

通过对相同等效能量密度的脉冲串模式飞秒激光和传统模式飞秒激光的消蚀结果进行比较分析，探究以上两种飞秒激光模式下实验样本消蚀效果的差异和对应的影响因素。

3 实验结果与讨论

3.1 脉冲串飞秒激光消蚀结果与分析

实验采用脉冲串模式飞秒激光进行血凝块样本消蚀，实验组 1～6 的实验结果如图 3 和图 4 所示。根据图 3 所示的显微图像，消蚀坑边缘不存在烧焦痕迹，且消蚀边缘与矩形扫描图案一致，未出现扭曲变形现象，消蚀坑周围也未出现因温度升高而导致的血凝块水分蒸发引起的塌陷，说明消蚀过程中未出现明显的热效应。

根据超景深三维显微镜获取的三维信息，提取平行于消蚀坑横边的中心纵剖面轮廓为消蚀坑形貌数据，如图 4 所示。在较高的等效能量密度下，提升等效能量密度对消蚀深度的增加效果不明显，如图 4(a)、(d)所示，消蚀深度的提升不超过 100 μm，但在

表 1 消蚀实验分组

Table 1 Ablation experimental groups

Experimental group No.	Pulse/burst energy /μJ	Repetition rate /kHz	Scan speed /(mm·s^{-1})	Equivalent energy density /(J·cm^{-2})
1	5×40	1	1	180.0
2			10	18.0
3			100	1.8
4		2	1	360.0
5			10	36.0
6			100	3.6
7	40	5	1	180.0
8			10	18.0
9			100	1.8
10		10	1	360.0
11			10	36.0
12			100	3.6

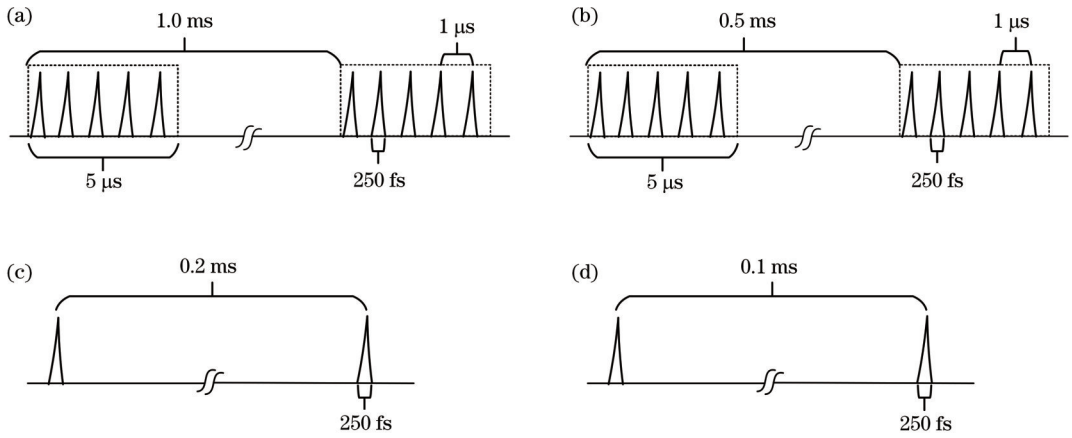

图 2 实验中使用的激光脉冲的重复频率的示意图。(a)实验组 1～3;(b)实验组 4～6;(c)实验组 7～9;(d)实验组 10～12

Fig. 2 Schematic diagrams of repetition rates of laser pulses used in experiments. (a) Experimental groups 1-3; (b) experimental groups 4-6; (c) experimental groups 7-9; (d) experimental groups 10-12

图 4(b)、(e)和图 4(c)、(f)之间大体上实现了提升一倍深度的效果,与等效能量密度的线性关系较好。该现象可能与振镜输出的聚焦照射光束的瑞利长度有关:实验组 2、3、5、6 的消蚀坑深度不超过光束的瑞利长度,消蚀坑底部平整,故实际照射的等效能量密度符合实验预设值;实验组 1、4 的消蚀坑过深(1000 μm 左右)并且在坑底出现了突出型结构,故坑底深度可能超过了瑞利长度,此时在坑底的实际等效能量密度与实验预设值不符,应低于实验预设值。从整体形状上来看,脉冲串模式飞秒激光产生的消蚀坑锥度小,有助于提升在手术中对血栓的清除率,并且在低能量密度范围内,消蚀坑深度与等效能量密度线性关系较好,便于通过调整激光参数来获得预期的消蚀深度。消蚀坑边缘处曲线的斜率变化率最大,故取消蚀坑曲线二阶导数绝对值最大值的位置作为边缘位置,消蚀坑曲线中有两个边缘点,取两个边缘点至消蚀坑底部垂直距离的均值为消蚀坑深度,作为后续拟合数据。

3.2 传统脉冲模式飞秒激光消蚀结果与分析

为比较脉冲串模式和传统脉冲模式间的差异,进行传统模式飞秒激光的消蚀实验,对应的实验组 7～12 的实验结果如图 5 和图 6 所示。在传统脉冲模式下,消蚀坑边缘同样不存在烧焦痕迹,如图 5 所示,但从显微图像的颜色深度来看,在相同光照条件下,图 5(b)、(e)的消蚀坑颜色明显浅于图 4(b)、(e),且在俯视视角下能够观察到图 5(b)、(e)中消蚀坑的斜坡内壁,故传统脉冲模式的消蚀深度应低于脉冲串模式,且具有更大的锥度。

将图 6 的消蚀坑轮廓数据与图 4 进行比较发现,在相同等效能量密度下,脉冲串模式的消蚀深度更深,以实验组 5、11 为例,等效能量密度均为 36 J/cm^2,但前者的消蚀深度是后者的 1.4 倍,说明脉冲串模式飞秒激光的消蚀效率更高。消蚀坑深度数据显示,即使消蚀深度没有超过聚焦光束的瑞利长度,传统脉冲模式下的消蚀深度与等效能量密度的线性关系仍然不明显,

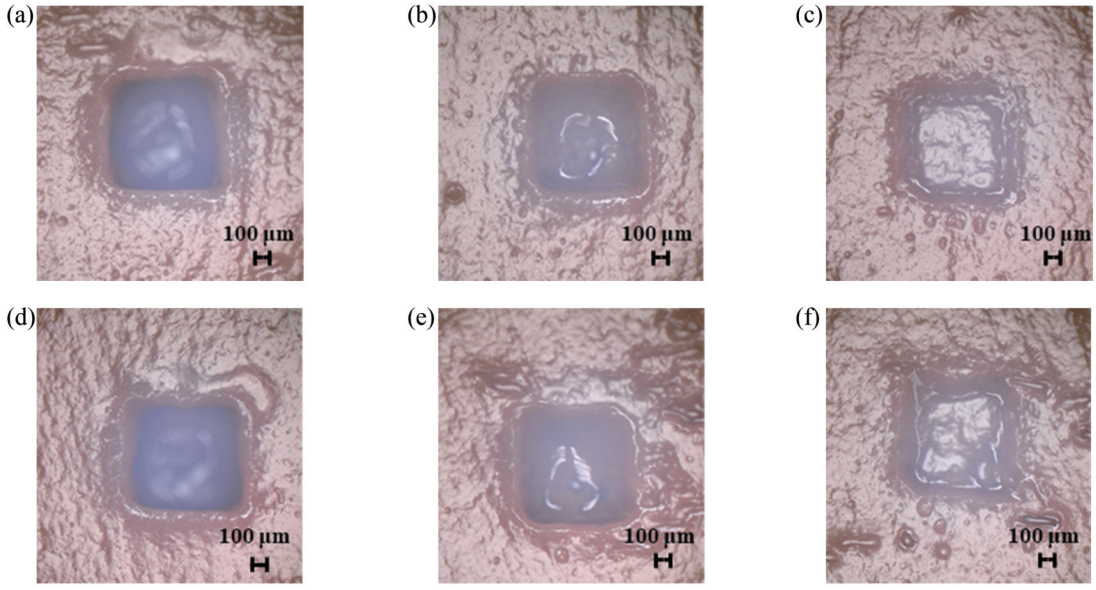

图 3 使用脉冲串模式飞秒激光获得的消蚀坑显微图像。(a)实验组 1;(b)实验组 2;(c)实验组 3;(d)实验组 4;(e)实验组 5;(f)实验组 6

Fig. 3 Microscopic images of ablation pits obtained by burst-mode femtosecond laser. (a) Experimental group 1; (b) experimental group 2; (c) experimental group 3; (d) experimental group 4; (e) experimental group 5; (f) experimental group 6

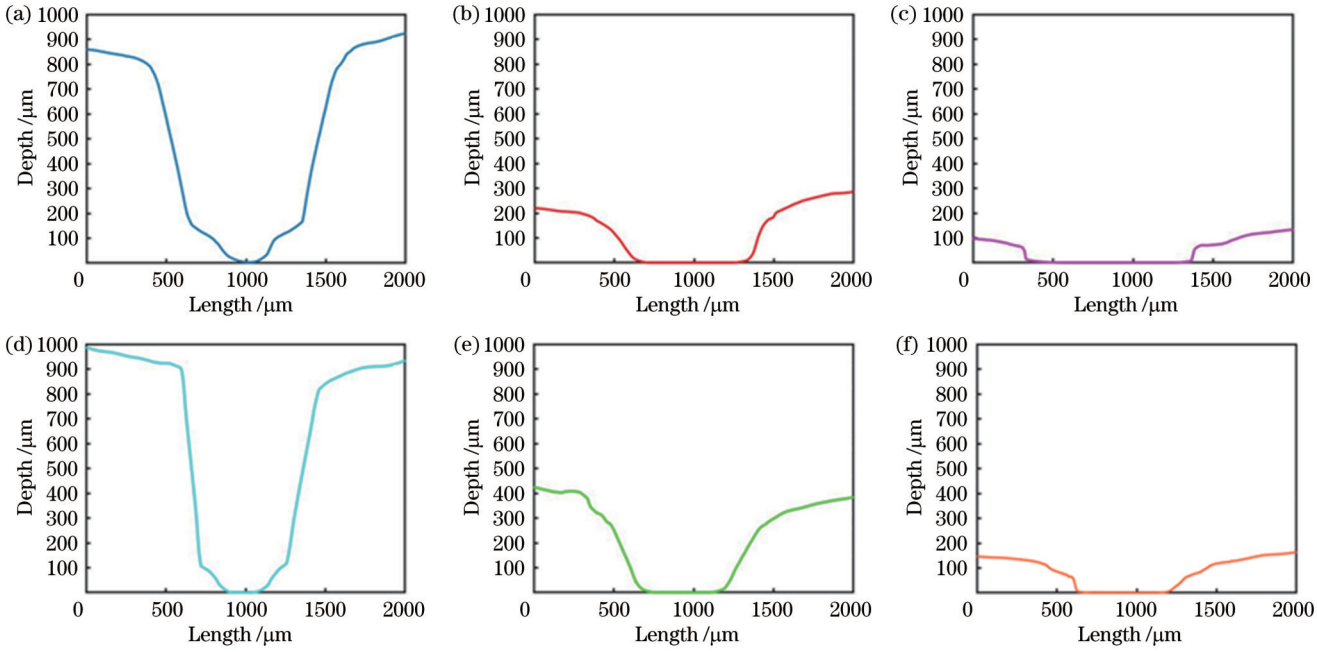

图 4 使用脉冲串模式飞秒激光获得的消蚀坑形貌数据。(a)实验组 1;(b)实验组 2;(c)实验组 3;(d)实验组 4;(e)实验组 5;(f)实验组 6

Fig. 4 Morphology data of ablation pits obtained by burst-mode femtosecond laser. (a) Experimental group 1; (b) experimental group 2; (c) experimental group 3; (d) experimental group 4; (e) experimental group 5; (f) experimental group 6

提升等效能量密度不能显著增加消蚀深度。从消蚀坑形状来看:实验组 7、10 的消蚀坑底部已经出现突出型结构,说明已经出现离焦现象;与实验组 2、5 的消蚀坑相比,实验组 8、11 的消蚀坑中出现明显斜坡且锥度更大,在手术中可能导致血栓清除率降低。

3.3 消蚀阈值拟合分析

经计算得到本实验系统聚焦光束的瑞利长度约为 1000 μm,故实验组 4、10 的消蚀坑底部处于严重离焦状态,对这两组数据进行舍弃处理。本实验已通过独立样本 T 检验证实实验数据差异具有统计学意义(显著性检验概率 $p<0.05$)。以消蚀坑深度数据为测定阈值的依据,对实验数据进行拟合处理,拟合结果如图 7 所示。由拟合结果可知:传统模式和脉冲串模式拟合曲线所推算出的消蚀阈值分别约为 1.093 J/cm^2 和

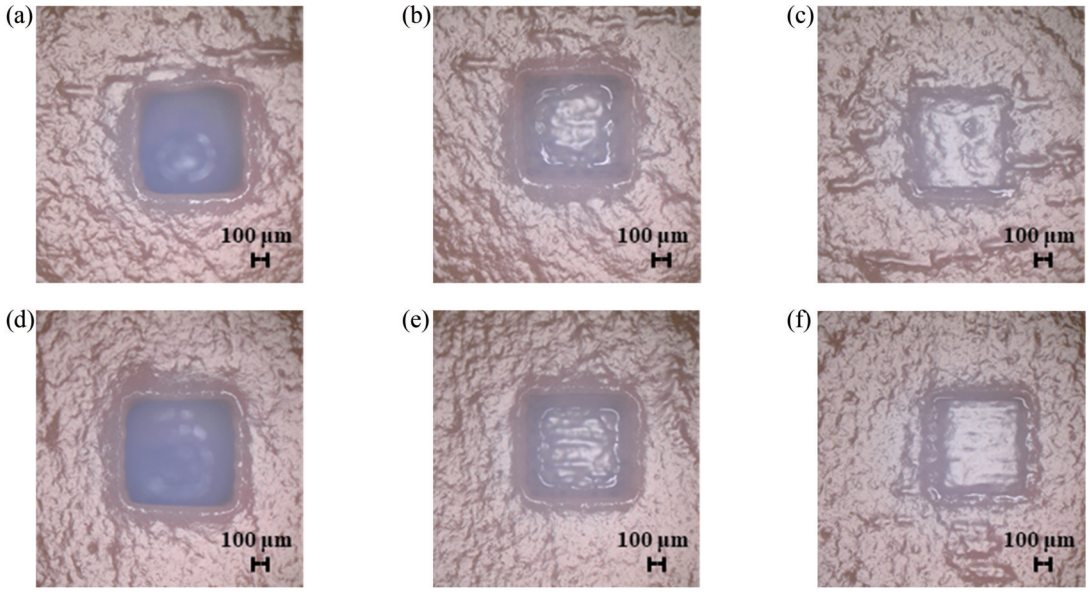

图 5 使用传统模式飞秒激光获得的消蚀坑显微图像。(a)实验组 7;(b)实验组 8;(c)实验组 9;(d)实验组 10;(e)实验组 11;(f)实验组 12

Fig. 5 Microscopic images of ablation pits obtained by traditional mode femtosecond laser. (a) Experimental group 7; (b) experimental group 8; (c) experimental group 9; (d) experimental group 10; (e) experimental group 11; (f) experimental group 12

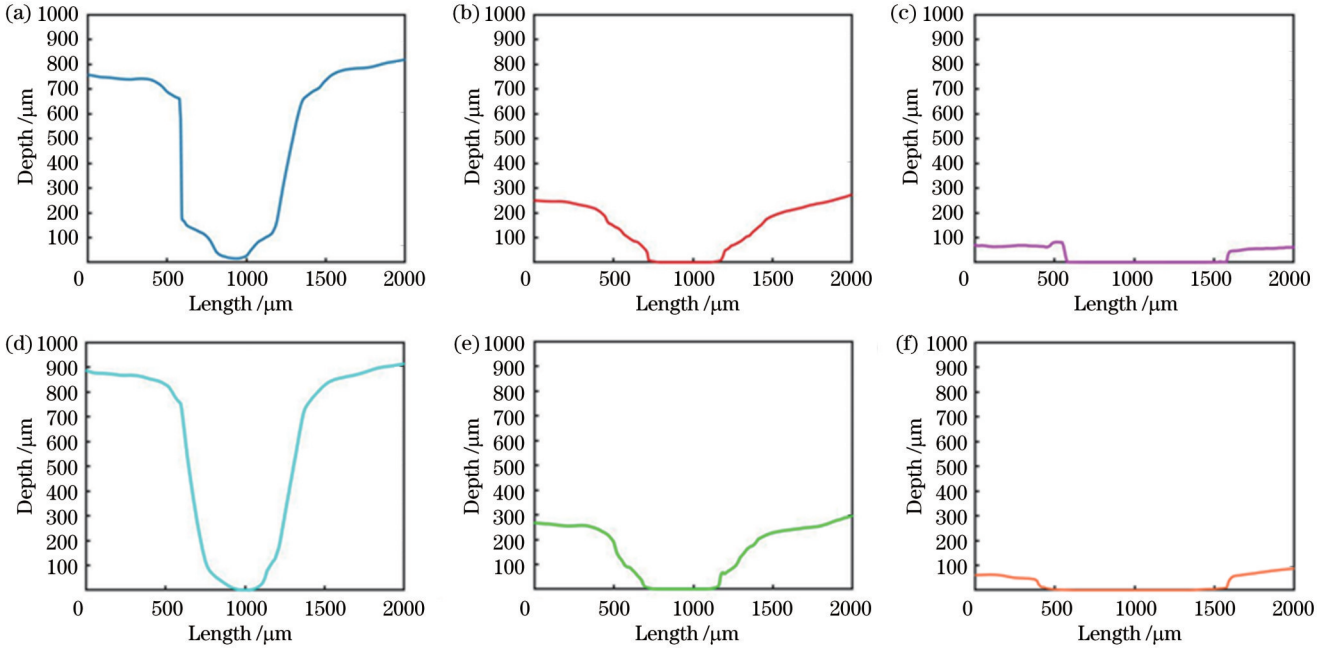

图 6 使用传统模式飞秒激光获得的消蚀坑形貌数据。(a)实验组 7;(b)实验组 8;(c)实验组 9;(d)实验组 10;(e)实验组 11;(f)实验组 12

Fig. 6 Morphology data of ablation pits obtained by traditional mode femtosecond laser. (a) Experimental group 7; (b) experimental group 8; (c) experimental group 9; (d) experimental group 10; (e) experimental group 11; (f) experimental group 12

0.104 J/cm^2,传统模式的消蚀阈值约为脉冲串模式的 10.5 倍;当消蚀深度均为 250 μm 时,传统模式需要的能量密度为 31.87 J/cm^2,而脉冲串模式则需要 19.19 J/cm^2,即仅需要脉冲模式 6/10 的脉冲能量即可实现相同的消蚀效率,故脉冲串飞秒激光可有效降低消蚀阈值,从而减少激光能量在组织内的沉积,抑制热损伤的产生,并提升消蚀效率。

对于脉冲串引起阈值降低和消蚀效率升高的原因,孵化现象是一种合理的解释,即脉冲串内先前脉冲对后续脉冲的作用产生了影响[27]。这种影响主要表现在两方面:吸收特性和能量沉积。在吸收特性方面:先前的脉冲会改变血凝块的表面形貌,表面吸收系数增大,从而增强了血凝块对激光能量的吸收,降低了消蚀阈值并提高了消蚀效率;另一种改变吸收特性的因素

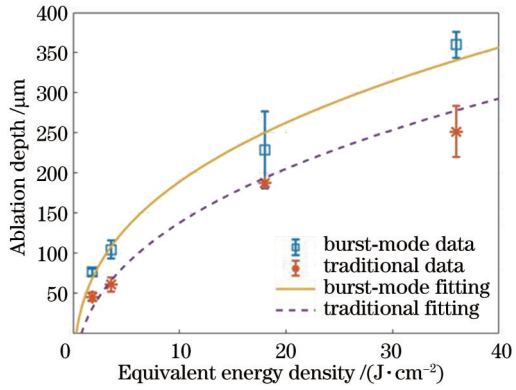

图 7 消蚀实验数据拟合结果

Fig. 7 Fitting results of ablation experimental data

是飞秒激光在血栓表面引起的电离，电离产生的自由电子会对激光能量产生强吸收，但该种自由电子的寿命仅为飞秒至皮秒量级[6]，远小于本文脉冲串内子脉冲的间隔，故该种情况不予考虑。在能量沉积方面，主要是照射区域局部热效应的沉积，虽然单个子脉冲的消蚀效果有限甚至无法产生消蚀效果，但是会改变血栓表面的局部初始温度，后续脉冲的到来可产生叠加效果，直到达到消蚀阈值发生消蚀，从而实现以多个低能量子脉冲实现消蚀的效果，降低了消蚀阈值并提高了消蚀效率。

4 结 论

使用鸭血凝块作为消蚀样本，分别使用脉冲串模式飞秒激光和传统脉冲模式飞秒激光进行消蚀实验并比较消蚀效果。实验发现，与传统脉冲模式飞秒激光相比，在相同能量密度下，脉冲串模式飞秒激光具有更高的消蚀效率、更小的消蚀坑锥度，有利于提高手术中的血栓清除率，并可显著降低消蚀阈值，抑制热损伤发生。在瑞利长度内，脉冲串模式飞秒激光的能量密度与消蚀深度具有更好的线性关系，有助于通过调整激光参数控制预期消蚀深度。因此，脉冲串模式飞秒激光消蚀血凝块具有安全、高效的特性，有望成为一种新型血栓清除技术。在进一步的研究中，计划采用红外热像仪等设备直接实时记录温度，并通过人体血栓模型、血管壁组织和动物实验等进一步验证脉冲串模式飞秒激光的高效性和安全性。

参 考 文 献

[1] Colling M E, Tourdot B E, Kanthi Y. Inflammation, infection and venous thromboembolism[J]. Circulation Research, 2021, 128(12): 2017-2036.

[2] Ebben H P, Jongkind V, Wisselink W, et al. Catheter directed thrombolysis protocols for peripheral arterial occlusions: a systematic review[J]. European Journal of Vascular and Endovascular Surgery, 2019, 57(5): 667-675.

[3] Shen Y, Wang X, Jin S S, et al. Increased risk of acute kidney injury with percutaneous mechanical thrombectomy using AngioJet compared with catheter-directed thrombolysis[J]. Journal of Vascular Surgery: Venous and Lymphatic Disorders, 2019, 7(1): 29-37.

[4] Fiorucci B, Isernia G, Simonte G, et al. Rheolytic thrombectomy with AngioJet® is safe and effective in revascularization of renal arteries′ acute occlusion on previous complex aortic endovascular repair[J]. Annals of Vascular Surgery, 2017, 45: 270.e1-270.e6.

[5] Tu T, Toma C, Tapson V F, et al. A prospective, single-arm, multicenter trial of catheter-directed mechanical thrombectomy for intermediate-risk acute pulmonary embolism: the FLARE study[J]. JACC: Cardiovascular Interventions, 2019, 12(9): 859-869.

[6] Rethfeld B, Ivanov D S, Garcia M E, et al. Modelling ultrafast laser ablation[J]. Journal of Physics D: Applied Physics, 2017, 50(19): 193001.

[7] Zhang J R, Guan K, Zhang Z, et al. *In vitro* evaluation of ultrafast laser drilling large-size holes on sheepshank bone[J]. Optics Express, 2020, 28(17): 25528-25544.

[8] Vogel A, Venugopalan V. Mechanisms of pulsed laser ablation of biological tissues[J]. Chemical Reviews, 2003, 103(2): 577-644.

[9] Kamlage G, Bauer T, Ostendorf A, et al. Deep drilling of metals by femtosecond laser pulses[J]. Applied Physics A, 2003, 77(2): 307-310.

[10] 崔梦雅, 黄婷, 肖荣诗. 基于纳米颗粒热效应的飞秒激光高效直写金属铜微结构[J]. 中国激光, 2022, 49(8): 0802015.
Cui M Y, Huang T, Xiao R S. Femtosecond laser direct writing of copper microstructures with high efficiency via thermal effect of nanoparticles[J]. Chinese Journal of Lasers, 2022, 49(8): 0802015.

[11] 赵强, 万辉, 于圣韬, 等. 飞秒激光制备柔性纳米多孔 Ag 材料的研究[J]. 中国激光, 2021, 48(8): 0802009.
Zhao Q, Wan H, Yu S T, et al. Investigation of flexible nanoporous silver materials fabricated by femtosecond laser[J]. Chinese Journal of Lasers, 2021, 48(8): 0802009.

[12] Bärsch N, Körber K, Ostendorf A, et al. Ablation and cutting of planar silicon devices using femtosecond laser pulses[J]. Applied Physics A, 2003, 77(2): 237-242.

[13] 郭恒, 闫剑锋, 李欣, 等. 空间整形飞秒激光图案化加工氧化石墨烯[J]. 中国激光, 2021, 48(2): 0202018.
Guo H, Yan J F, Li X, et al. Patterned graphene oxide by spatially-shaped femtosecond laser[J]. Chinese Journal of Lasers, 2021, 48(2): 0202018.

[14] Chung S H, Mazur E. Surgical applications of femtosecond lasers[J]. Journal of Biophotonics, 2009, 2(10): 557-572.

[15] 胡昕宇, 马卓晨, 韩冰, 等. 飞秒激光制备蛋白质智能软体执行器[J]. 中国激光, 2021, 48(14): 1402001.
Hu X Y, Ma Z C, Han B, et al. Femtosecond laser fabrication of protein-based smart soft actuators[J]. Chinese Journal of Lasers, 2021, 48(14): 1402001.

[16] 陈列, 聂琦璐, 郭飞, 等. 飞秒激光刻蚀硅橡胶超疏水表面老化特征的研究[J]. 中国激光, 2022, 49(10): 1002606.
Chen L, Nie Q L, Guo F, et al. Aging characteristics of superhydrophobic silicone rubber surfaces etched by femtosecond laser[J]. Chinese Journal of Lasers, 2022, 49(10): 1002606.

[17] Momma C, Chichkov B N, Nolte S, et al. Short-pulse laser ablation of solid targets[J]. Optics Communications, 1996, 129(1/2): 134-142.

[18] Lorazo P, Lewis L J, Meunier M. Short-pulse laser ablation of solids: from phase explosion to fragmentation[J]. Physical Review Letters, 2003, 91(22): 225502.

[19] Marjoribanks R S, Dille C, Schoenly J E, et al. Ablation and thermal effects in treatment of hard and soft materials and biotissues using ultrafast-laser pulse-train bursts[J]. Photonics & Lasers in Medicine, 2012, 1(3): 155-169.

[20] Herman P R, Oettl A, Chen K P, et al. Laser micromachining of transparent fused silica with 1-ps pulses and pulse trains[J].

Proceedings of SPIE, 1999, 3616: 148-155.
[21] Ma N, Chen M, Yang C, et al. High-efficiency 50 W burst-mode hundred picosecond green laser[J]. High Power Laser Science and Engineering, 2020, 8(1): 5-10.
[22] Butkus S, Jukna V, Paipulas D, et al. Micromachining of invar foils with GHz, MHz and kHz femtosecond burst modes[J]. Micromachines, 2020, 11(8): 733.
[23] Kalaycıoğlu H, Elahi P, Akçaalan Ö, et al. High-repetition-rate ultrafast fiber lasers for material processing[J]. IEEE Journal of Selected Topics in Quantum Electronics, 2018, 24(3): 8800312.
[24] Račiukaitis G. Ultra-short pulse lasers for microfabrication: a review[J]. IEEE Journal of Selected Topics in Quantum Electronics, 2021, 27(6): 1100112.
[25] Elahi P, Akçaalan Ö, Ertek C, et al. High-power Yb-based all-fiber laser delivering 300 fs pulses for high-speed ablation-cooled material removal[J]. Optics Letters, 2018, 43(3): 535-538.
[26] Kerse C, Kalaycıoğlu H, Elahi P, et al. Ablation-cooled material removal with ultrafast bursts of pulses[J]. Nature, 2016, 537(7618): 84-88.
[27] Sun Z L, Lenzner M, Rudolph W. Generic incubation law for laser damage and ablation thresholds[J]. Journal of Applied Physics, 2015, 117(7): 073102.

Blood Clot Ablation Effects Based on Burst-Mode Femtosecond Laser

Liu Xiaozheng[1], Li Younan[2], Zhang Haitao[3**], Gu Ying[1,4*], Wu Weiwei[2], Zhang Tong[2]

[1]*School of Optics and Photonics, Beijing Institute of Technology, Beijing* 100081, *China*;
[2]*Department of Vascular Surgery, Affiliated Beijing Tsinghua Changgung Hospital, School of Clinical Medicine, Tsinghua University, Beijing* 102218, *China*;
[3]*Key Laboratory of Photonic Control Technology, Ministry of Education, Center for Photonics and Electronics, Department of Precision Instrument, Tsinghua University, Beijing* 100084, *China*;
[4]*Department of Laser Medicine, First Medical Center of PLA General Hospital, Beijing* 100853, *China*

Abstract

Objective Thromboembolism and thrombosis are the important causes of arterial occlusive diseases. Rapid thrombus removal is one of the key strategies in the treatment of arterial thrombotic diseases. Currently, the most thrombus removal is achieved through surgery. However, conventional thrombus removal procedures, such as open surgery and minimally invasive surgery, have low thrombus removal rate and the risk of vessel wall damage and rupture. As a new laser technology, the burst-mode femtosecond laser has the potential to solve these problems. It shows low thermal effect and high ablation efficiency in industrial precision machining, which is expected to provide a new solution for thrombus removal technology. However, there is a lack of experimental data to verify the actual ablation effects on thrombus with the burst-mode femtosecond laser. The ablation effect with the burst-mode femtosecond laser based on animal blood clot samples is studied in this paper. The experimental results show that the burst-mode femtosecond laser improves the ablation efficiency and reduces the ablation threshold, which has great clinical research and development potential.

Methods In this study, the ablation experimental platform is established with femtosecond laser and high-speed galvanometer. The laser can output both traditional mode pulses and burst-mode pulses, and the repetition rate is adjustable. In addition, a pair of aperture stops and a pair of reflectors are set in the platform to adjust beam diameter and fold optical path, respectively. The fresh edible duck blood clots purchased in the market are used as ablation samples. During the ablation experiments, the glass tube containing the blood clot samples is inserted into the sample bracket fixed on the z-axis lifting platform. To facilitate detection and observation, a single-layer large-area scanning method is proposed to carry out the ablation experiments. According to repetition rate, pulse energy, scanning speed, and pulse output mode, 12 experimental groups are set up. The three-dimensional super depth of field microscope is adopted to observe and record the images and data of ablation pits. The ablation threshold is obtained by fitting multiple groups of experimental data. Through the comparison and analysis of the ablation results with burst-mode femtosecond laser and traditional mode femtosecond laser in the same equivalent energy density, the differences in the ablation effects under the above two modes are explored.

Results and Discussions In the ablation experiments with the burst-mode femtosecond laser, no burn marks occur on the edge of the ablation pit (Fig. 3). The ablation edge is consistent with the rectangular scanning pattern without distortion. There is no collapse caused by rising temperatures and water evaporation around the ablation pit, which shows that no obvious thermal effects appear in the process of ablation. From the perspective of the shape of the ablation pit, the taper of the ablation pit generated by the burst-mode femtosecond laser is small (Fig. 4), which is conducive to improving the thrombus removal rate during surgery. Moreover, the linear relationship between the depth of the ablation pit and the

equivalent energy density is great in the range of low energy density, which is convenient to obtain the expected ablation depth by adjusting the laser parameters. Compared with that of the burst-mode femtosecond laser, the ablation depth of the traditional mode femtosecond laser is smaller under the same equivalent energy density. Additionally, there are obvious slopes and large taper in the ablation pit, which may lead to reduced thrombus clearance rate during surgery. The ablation thresholds calculated by the fitting curves of the traditional mode and the burst mode are about 1.093 J/cm^2 and 0.104 J/cm^2, respectively. The ablation threshold of the traditional mode is about 10.5 times that of the burst mode. The energy density required to obtain 250 μm ablation depth with the traditional mode is 31.87 J/cm^2, while that with the burst mode is only 19.19 J/cm^2. Therefore, the burst-mode femtosecond laser can effectively reduce the ablation threshold and improve the ablation efficiency.

Conclusions In this paper, the ablation effects of burst-mode femtosecond laser and traditional mode femtosecond laser are analyzed. Compared with the traditional mode femtosecond laser, under the same energy density, the burst-mode femtosecond laser has higher ablation efficiency and smaller ablation pit taper, which is beneficial to improving the thrombus removal rate. The ablation thresholds calculated by the fitting curves of the traditional mode and the burst mode are about 1.093 J/cm^2 and 0.104 J/cm^2, respectively. The ablation threshold of the traditional mode is about 10.5 times that of the burst mode. In Rayleigh length, the energy density of burst-mode femtosecond laser has a great linear relationship with the ablation depth, which is helpful to control the expected ablation depth by adjusting the laser parameters. This study shows that the burst-mode femtosecond laser has great clinical research and development potential to become a novel type of thrombus removal technology.

Key words medical optics; femtosecond laser; tissue ablation; burst mode; three-dimensional microscopic imaging